Journal of Molecular Cell Biology (2024), 16(11), mjae051 https://doi.org/10.1093/jmcb/mjae051
Published online January 23, 2025

Article

Low-dose quinine targets KCNH6 to potentiate glucose-induced insulin secretion

Feng-Ran Xiong[1,2], Juan-Juan Zhu[1,2], Xiao-Rong Zhu[1,2], Jing Lu[1,2,*], and Jin-Kui Yang[1,2,*]

[1] Department of Endocrinology, Beijing Diabetes Institute, Beijing Key Laboratory of Diabetes Research and Care, Beijing Tongren Hospital, Capital Medical University, Beijing 100730, China
[2] Laboratory for Clinical Medicine, Capital Medical University, Beijing 100069, China
* Correspondence to: Jing Lu, E-mail: jinglu_tr@ccmu.edu.cn; Jin-Kui Yang, E-mail: jkyang@ccmu.edu.cn

Edited by Feng Liu

Insulin secretion is mainly regulated by two electrophysiological events, depolarization initiated by the closure of adenosine triphosphate (ATP)-sensitive K^+ (K_{ATP}) channels and repolarization mediated by K^+ efflux. Quinine, a natural component commonly used for the treatment of malaria, has been reported to directly stimulate insulin release and lead to hypoglycemia in patients during treatment through inhibiting K_{ATP} channels. In this study, we verified the insulinotropic effect of quinine on the isolated mouse pancreatic islets. We also revealed that low-dose quinine (<20 μM) did not directly provoke Ca^{2+} spikes or insulin secretion under low-glucose conditions but potentiated Ca^{2+} influx and insulin secretion induced by high glucose, which cannot be explained by K_{ATP} inhibition. KCNH6 (hERG2) is a voltage-dependent K^+ (Kv) channel that plays a critical role in the repolarization of pancreatic β cells. Patch clamp experiments showed that quinine inhibited hERG channels at low micromolar concentrations. However, whether quinine can target KCNH6 to potentiate glucose-induced insulin secretion remains unclear. Here, we showed that *in vivo* administration of low-dose quinine (25 mg/kg) improved glucose tolerance and increased glucose-induced insulin release in wild-type control mice but not in *Kcnh6*-β-cell-specific knockout (βKO) mice. Consistently, *in vitro* treatment of primary islet β cells with low-dose quinine (10 μM) prolonged action potential duration and augmented glucose-induced Ca^{2+} influx in the wild-type control group but not in the *Kcnh6*-βKO group. Our results demonstrate that KCNH6 plays an important role in low-dose quinine-potentiated insulin secretion and provide new insights into KCNH6-targeted drug development.

Keywords: quinine, insulin secretion, KCNH6

Introduction

Quinine, an alkaloid derived from the bark of the cinchona tree, has long been used as a first-line active antimalarial agent (Achan et al., 2011). Among patients treated with quinine for malaria, a high incidence of hypoglycemia has been observed in many studies (Harats et al., 1984; Jones et al., 1986; Kerr and Bdiri, 2008). The amount of insulin secreted is directly associated with the electrical activity of β cells, which is controlled by multiple ion channels. The closure of adenosine triphosphate (ATP)-sensitive K^+ (K_{ATP}) channels evokes the depolarization of pancreatic β cells, which is the initial step of insulin secretion (Misler et al., 1989, 1992). As a result, K_{ATP} channel has been identified as a classic target of insulin secretagogues such as sulfonylureas (Proks et al., 2002; Bryan et al., 2005). The association between quinine and hypoglycemia is mainly attributed to the drug directly stimulating insulin release by inhibiting K_{ATP} (Henquin, 1982; Gribble et al., 2000). In addition to K_{ATP} channels, voltage-dependent K^+ (K_V) channels also participate in insulin secretion by mediating the repolarization of β cells to rest potential (Jacobson and Philipson, 2007). Therefore, as a broad-spectrum K^+ channel blocker (Fatherazi and Cook, 1991), quinine may also promote insulin secretion through inhibiting the repolarizing K^+ channel, which has been less studied.

QT interval prolongation, another severe side effect arising during treatment with quinine (Saadeh et al., 2022), results from blocking human ether-a-go-go-related gene (hERG) K^+ channels, which have three subtypes, hERG1 (KCNH2), hERG2 (KCNH6), and hERG3 (KCNH7) channels (Shi et al., 1997). Mutations in KCNH6 have been shown to be associated with congenital hyperinsulinism of infancy via a whole-exome sequencing analysis

Received July 2, 2024. Revised October 27, 2024. Accepted January 22, 2025.

(Proverbio et al., 2013). Our previous study revealed that loss-of-function mutations in KCNH6 lead to neonatal hyperinsulinemia in humans and mice (Yang et al., 2018). Considering that quinine was reported to inhibit hERG channels at low micromolar concentrations in CHO cells (Dierich et al., 2019), we hypothesize that KCNH6 inhibition plays an important role in quinine-mediated excessive insulin secretion in pancreatic β cells.

Here, we demonstrated that low-dose quinine did not provoke Ca^{2+} spikes or insulin secretion under low-glucose conditions but promoted the glucose-stimulated insulin secretion (GSIS) via high glucose-evoked increase in intracellular Ca^{2+} levels, which cannot be explained by K_{ATP} inhibition. *Kcnh6*-β-cell-specific knockout (βKO) mice were used for *in vivo* and *in vitro* experiments to investigate the targets of low-dose quinine. We found that low-dose quinine increased glucose-induced insulin release, prolonged action potential duration (APD), and augmented glucose-induced Ca^{2+} influx in wild-type (WT) control mice but not in *Kcnh6*-βKO mice, suggesting that KCNH6 plays a crucial role in quinine-potentiated insulin secretion.

Results

Low-dose quinine promotes insulin secretion induced by high glucose

Hypoglycemia is a widely known side effect of the antimalarial drug quinine, which is caused by the insulinotropic effect of the drug through the inhibition of K_{ATP} channels. To verify the role of quinine in insulin secretion, we performed a GSIS test using primary mouse islets treated with a wide range of quinine dosage (Figure 1A). Quinine potentiated high glucose (25 mM)-evoked insulin secretion in a dose-dependent manner at 5–100 μM. However, under low-glucose (2 mM) conditions, quinine induced insulin secretion only at concentrations of 50–100 μM; without the addition of glucose, 5 μM quinine alone was not sufficient to stimulate insulin secretion. The impaired insulin secretion of islets treated with 500 or 1000 μM quinine may result from the toxic effect of the drug on cell viability, as observed in the 3-(4,5-dimethylthiazol-2-yl)-2,5-diphenyl diphenyltetrazolium bromide (MTT) test (Figure 1C). We further narrowed down the drug concentration to 0–40 μM in the GSIS test (Figure 1B). Notably, 40 μM quinine induced insulin secretion under both low- and high-glucose conditions, whereas 2.5–20 μM quinine only promoted insulin release under high-glucose conditions, suggesting that low-dose quinine may potentiate insulin secretion by inhibiting other repolarizing K^+ channels that prolong the APD rather than by closing K_{ATP} channels. Ca^{2+} is the direct trigger of insulin secretion. Ca^{2+} imaging showed that low-dose (5, 10, and 20 μM) quinine was not sufficient to induce Ca^{2+} spikes under low-glucose conditions but enhanced the increase in intracellular Ca^{2+} levels evoked by high-glucose stimuli (Figure 1D and E). The dynamic perfusion test showed that islets perfused with 10 μM quinine exhibited greater insulin secretion under high-glucose stimuli than those perfused with vehicle control (DMSO) (Figure 1F). Based on these results, we concluded that low-dose quinine promotes insulin secretion induced by high glucose.

Quinine is an inhibitor of KCNH6 channels

We previously demonstrated that KCNH6 plays an important role in insulin secretion by participating in repolarizing β cells. Considering that quinine has been reported to inhibit KCNH2 channels in transfected CHO cells, we recruited HERG-null human embryonic kidney 293 (HEK293) cells, a commonly used model cell line to express non-endogenous ion channels (Fedida et al., 1996, 1997; Malin et al., 1998). After transfecting HEK293T cells with KCNH6 or KCNH2 gene, we applied increasing concentrations of quinine on the cells and compared the effects of quinine on the two channels in electrophysiological experiments. E4031 was used as an inhibitor control for both KCNH2 and KCNH6 (Figure 2A, B, F, and G). Patch clamp experiments showed that quinine inhibited the KCNH6 current in a concentration-dependent manner, with an IC_{50} of 2.123 μM and a Hill coefficient of 0.7427 (Figure 2H–J), while the IC_{50} of quinine on KCNH2 was calculated to be 4.775 μM (Figure 2C–E). These results indicated that quinine inhibits hERG channels at low micromolar concentrations and the affinity of quinine for KCNH6 channels was ∼2 times greater than that for KCNH2 channels.

Low-dose quinine increases insulin secretion and accelerates glucose clearance in WT and Kcnh2-βKO mice but not in Kcnh6-βKO mice

To confirm the insulinotropic effect of quinine *in vivo*, we administered increasing doses of quinine (25, 50, 100, and 200 mg/kg) to C57BL/6 J WT mice by oral gavage (Figure 3A) and performed insulin release test (IRT). Compared with those in the control group, mice in the 100 mg/kg and 200 mg/kg quinine groups exhibited significantly elevated plasma insulin levels, accompanied by decreased blood glucose levels, whereas mice in the 25 mg/kg or 50 mg/kg quinine groups did not show significant changes in insulin release (Figure 3B and C). However, when we applied 25 mg/kg quinine or vehicle (DMSO) 1 h before glucose administration (2 mg/kg, i.p.) in intraperitoneal glucose tolerance test (IPGTT) (Figure 3D), glucose-evoked insulin secretion was significantly elevated in the quinine-treated WT mice, followed by accelerated glucose clearance (Figure 3E and F). To investigate the drug target of quinine, 25 mg/kg quinine was administered to *Kcnh2*-βKO or *Kcnh6*-βKO mice 1 h before IPGTT. The glucose-evoked insulin release in *Kcnh2*-βKO mice was potentiated, along with a decrease in blood glucose level (Figure 3G and H), whereas both plasma insulin and blood glucose levels in *Kcnh6*-βKO mice were not altered by quinine administration (Figure 3I and J), suggesting that 25 mg/kg quinine potentiates high glucose-induced insulin release by targeting KCNH6 channels.

Low-dose quinine enhances the GSIS of islets and glucose-induced Ca^{2+} spikes in β cells from WT and Kcnh2-βKO mice but not from Kcnh6-βKO mice

We isolated islets from *Kcnh6*-βKO and *Kcnh2*-βKO mice and performed GSIS tests with 10 μM quinine. Consistent with the *in vivo* IRT results, 10 μM quinine significantly enhanced high

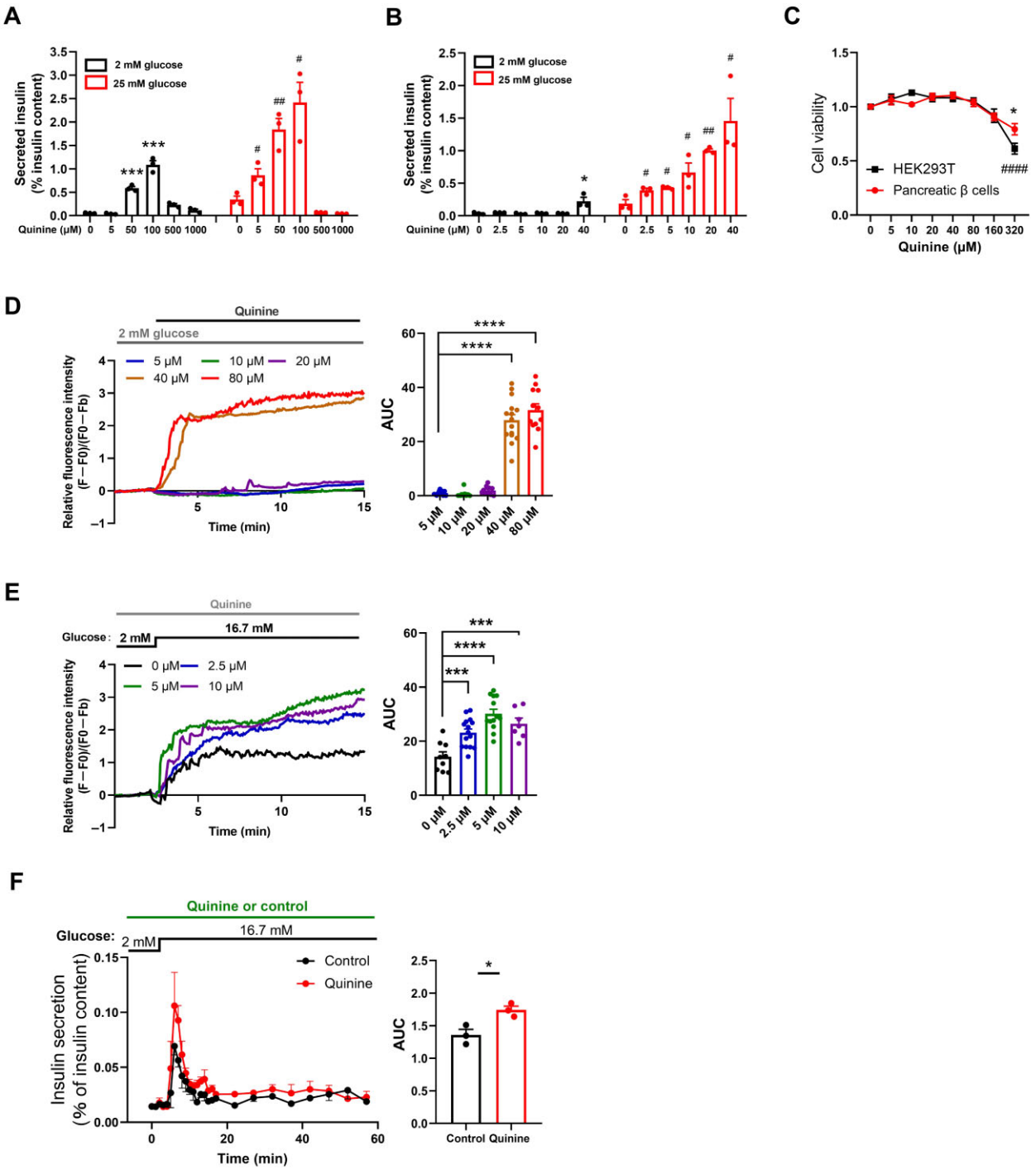

Figure 1 Low-dose quinine promotes insulin secretion induced by high glucose. (**A** and **B**) Normalized secreted insulin levels before and after high-glucose (25 mM) stimulation during a GSIS test with mouse islets in the presence of 0–1000 μM (**A**) or 0–40 μM (**B**) quinine as indicated. $n = 3$. $^{*}P < 0.05$ and $^{***}P < 0.001$ vs. the control at 2 mM glucose; $^{\#}P < 0.05$ and $^{\#\#}P < 0.01$ vs. the control at 25 mM glucose. (**C**) Viability of the indicated cells incubated with different concentrations of quinine for 24 h. $n = 3$ for pancreatic β cells, $^{*}P < 0.05$ vs. 0 μM quinine; $n = 6$ for HEK293T cells, $^{\#\#\#\#}P < 0.0001$ vs. 0 μM quinine. (**D**) Cytosolic Ca^{2+} transients upon the application of the indicated concentrations of quinine. $^{****}P < 0.0001$. (**E**) Glucose-stimulated increase in the intracellular Ca^{2+} concentration in the presence of different concentrations of quinine as indicated. $^{***}P < 0.001$ and $^{****}P < 0.0001$. (**F**) Normalized consecutive secreted insulin levels of islets (40 per lane) during high-glucose perfusion in the presence or absence of 10 μM quinine. $n = 3$. $^{*}P < 0.05$ vs. control. The values are presented as mean ± SEM. Significance values were calculated using Student's unpaired *t*-test.

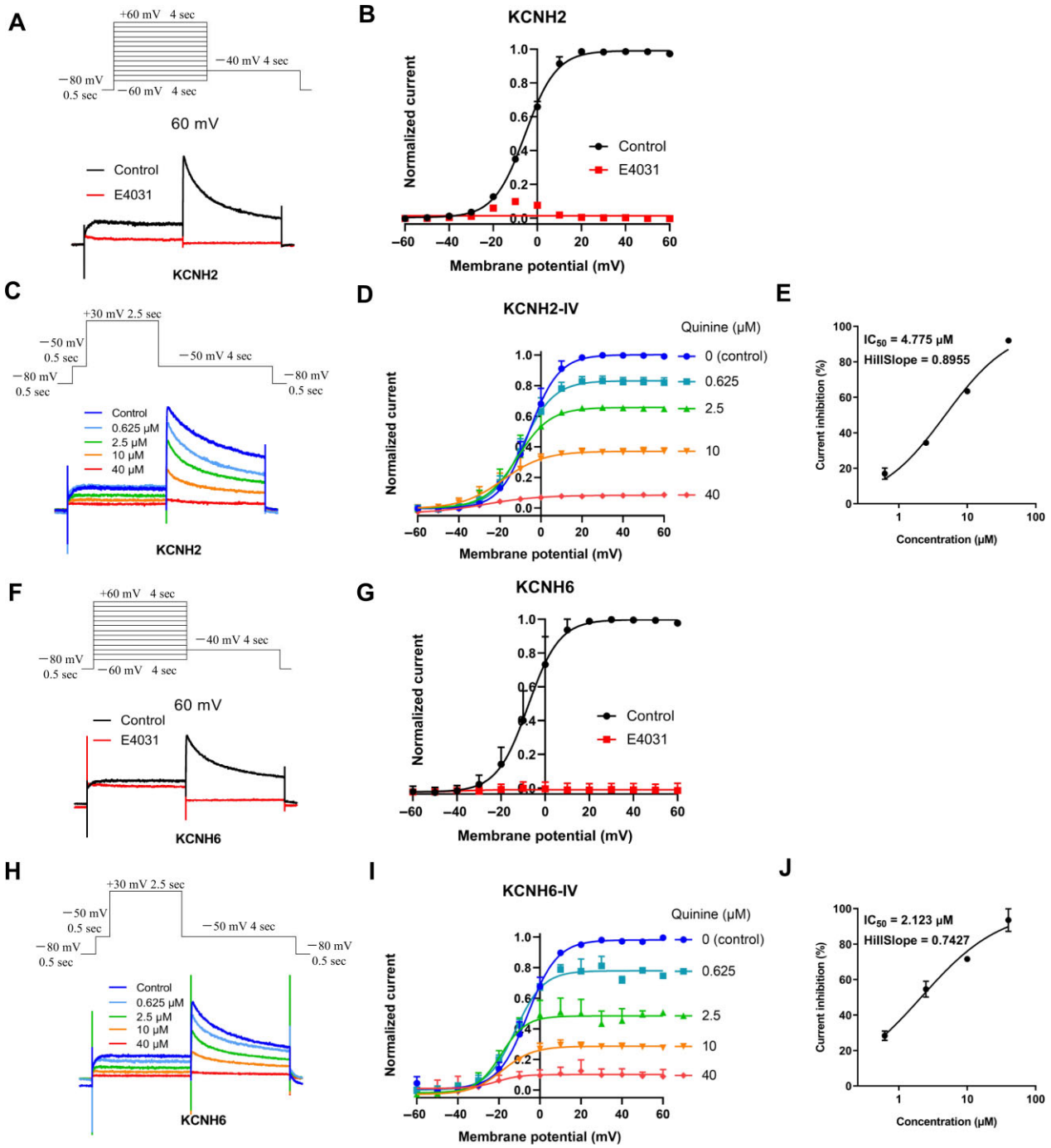

Figure 2 Effects of quinine on KCNH2 and KCNH6 currents in transfected HEK293T cells. (**A** and **F**) Representative whole-cell hERG currents in KCNH2- or KCNH6-transfected HEK293T cells in the absence or presence of E4031. (**B** and **G**) Current–voltage (I–V) curve for the normalized tail currents in KCNH2- or KCNH6-transfected HEK293T cells in the absence or presence of E4031, as measured from the peak currents. (**C** and **H**) Representative whole-cell hERG currents in KCNH2- or KCNH6-transfected HEK293T cells after the application of the indicated concentrations of quinine. (**D** and **I**) I–V curve for the normalized tail currents in KCNH2- or KCNH6-transfected HEK293T cells treated with different concentrations of quinine. (**E**) Dose-dependent effects of quinine on KCNH2 channel blockade. The IC_{50} was 4.775 μM, with a Hill coefficient of 0.8955. (**J**) Dose-dependent effects of quinine on KCNH6 channel blockade. The IC_{50} was 2.123 μM, with a Hill coefficient of 0.7427.

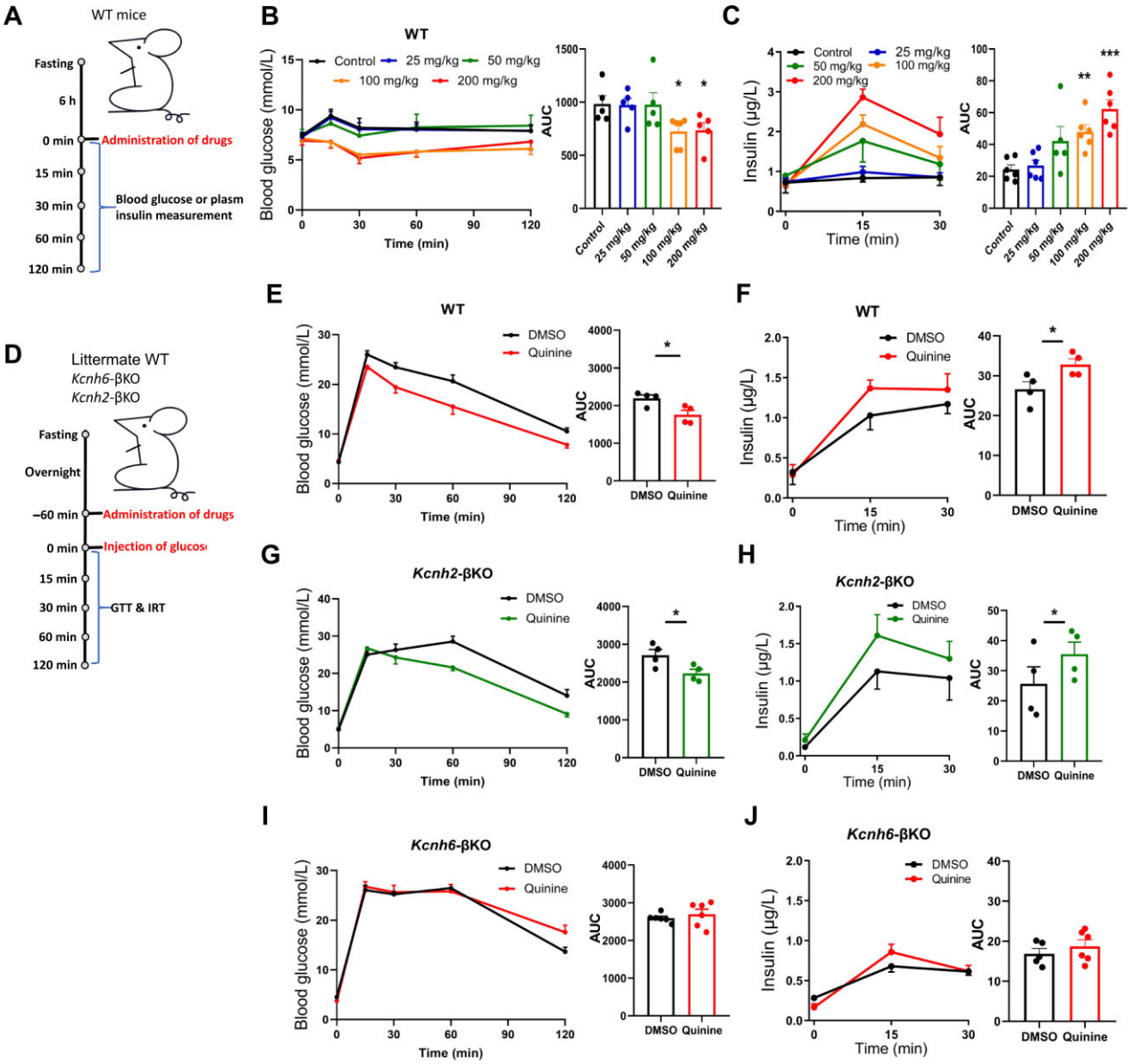

Figure 3 Insulinotropic effect of quinine *in vivo*. (**A**–**C**) WT mice were administered with quinine at different doses. (**A**) Flow chart depicting the experimental steps. (**B**) Blood glucose concentrations. (**C**) Plasma insulin concentrations. (**D**–**J**) WT, *Kcnh2*-βKO, and *Kcnh6*-βKO mice received i.p. injection of glucose after 1 h treatment with quinine or vehicle (DMSO). (**D**) Flow chart depicting the experimental steps. (**E** and **F**) Blood glucose and plasma insulin concentrations in WT mice. (**G** and **H**) Blood glucose and plasma insulin concentrations in *Kcnh2*-βKO mice. (**I** and **J**) Blood glucose and plasma insulin concentrations in *Kcnh6*-βKO mice. The values are presented as mean ± SEM. **P* < 0.05 vs. control or DMSO. Significance values were calculated using Student's unpaired *t*-test.

glucose-evoked insulin secretion of islets from WT and *Kcnh2*-βKO mice but not altered the insulin secretion of islets isolated from *Kcnh6*-βKO mice (Figure 4A, C, and E). To exclude the possibility that islets from *Kcnh6*-βKO mice were too fragile to react to any stimuli, we applied 10, 50, and 100 μM quinine to the islets isolated from WT and *Kcnh6*-βKO mice and compared insulin secretion (Figure 4G). Although quinine-induced insulin secretion of islets was impaired in *Kcnh6*-βKO mice compared to that in WT mice, 50 or 100 μM quinine was sufficient to evoke insulin secretion, indicating that the inaction of 10 μM quinine on insulin secretion indeed resulted from KCNH6 ablation. Furthermore, Ca^{2+} imaging using dispersed β cells from mice showed that 10 μM quinine elevated the glucose-induced Ca^{2+} spikes in β cells from WT and *Kcnh2*-βKO mice but not *Kcnh6*-βKO mice (Figure 4B, D, and F), confirming that KCNH6 is an important target of quinine in pancreatic islets.

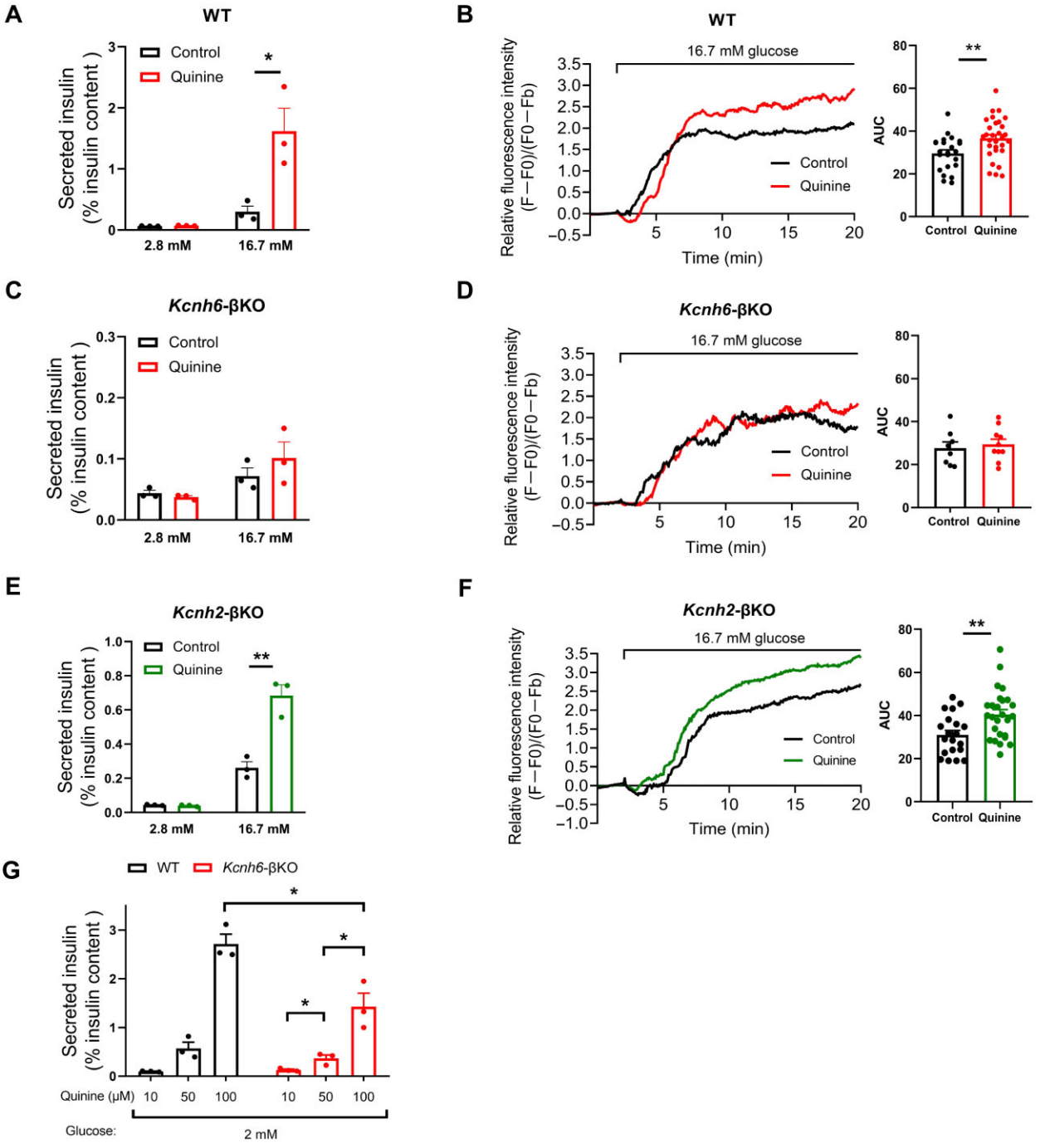

Figure 4 Effects of low-dose quinine on the GSIS and cytosolic Ca^{2+} transients in β cells *in vitro*. (**A**–**F**) Islets and primary islet β cells were isolated from WT, *Kcnh2*-βKO, and *Kcnh6*-βKO mice. (**A**, **C**, and **E**) Normalized secreted insulin levels in islets before and after high-glucose (16.7 mM) stimulation during a GSIS test. (**B**, **D**, and **F**) Glucose (16.7 mM)-evoked intracellular Ca^{2+} transients in primary islet β cells. The cytosolic Ca^{2+} concentration is represented by (F−F0)/(F0−Fb) of Fluo-4, where F0 is the baseline fluorescence and Fb is the background fluorescence. The calculated AUCs are shown next to the corresponding fluorescence intensity images. (**G**) Normalized insulin secretion of WT and βKO islets treated with different concentrations of quinine under low-glucose conditions. The values are presented as mean ± SEM. *$P < 0.05$ and **$P < 0.01$. Significance values were calculated using Student's unpaired *t*-test.

Undetected insulinotropic effect of low-dose quinine on high-fat diet (HFD)-fed Kcnh6-βKO mice in vivo and in vitro

We next investigated the glucose-lowering effect of quinine on HFD-fed hyperglycemic mice. Compared to the DMSO control, 25 mg/kg quinine accelerated glucose clearance and increased plasma insulin levels in HFD-fed WT mice (Figure 5A and B) but not in HFD-fed *Kcnh6*-βKO mice (Figure 5C and D). Consistently, 10 μM quinine, which significantly increased the GSIS of islets from HFD-fed WT mice, was not sufficient to change the insulin secretion of HFD-fed *Kcnh6*-βKO islets (Figure 5E and G). An increase in glucose-evoked Ca^{2+} spikes boosted by 10 μM quinine was only observed in the β cells from HFD-fed WT mice but not in the β cells from *Kcnh6*-βKO mice (Figure 5F and H). These results further indicated the important role of KCNH6 in the quinine-induced insulinotropic effect.

Chronic low-dose quinine administration improves metabolic parameters in mice

We also evaluated the chronic effect of low-dose quinine on several metabolic parameters in normal chow- or HFD-fed WT and *Kcnh6*-βKO mice (Figure 6A and J). In normal chow-fed mice, chronic low-dose quinine administration reduced blood glucose levels and enhanced plasma insulin levels in the WT but not the βKO group (Figure 6D, E, G, and H), consistent with the consequences of instant quinine administration. In HFD-fed mice, the potentiated insulin release was only observed in the WT but not the βKO group (Figure 6N and Q), while decreased blood glucose levels were observed in both WT and βKO groups after chronic treatment of low-dose quinine (Figure 6M and P). We then determined insulin sensitivity by performing insulin tolerance test (ITT) (Figure 6F, I, O, and R). The insulin sensitivity was improved in both HFD-fed WT and βKO mice after long-term quinine administration (Figure 6O and R), which explained the better glucose tolerance in βKO mice. In addition, we measured serum triglyceride (TG) and total cholesterol (TC) levels (Figure 6B, C, K, and L) and revealed that long-term quinine administration reduced TC levels in both HFD-fed WT and βKO mice. These results indicated that chronic low-dose quinine administration increases insulin secretion by targeting KCNH6 and the long-term effects of quinine to improve insulin intolerance and lipid homeostasis are independent of β-cell-specific KCNH6 knockout.

Differential electrophysiological responses to low-dose quinine between WT and Kcnh6-βKO primary β cells

Considering that 10 μM quinine cannot close enough K_{ATP} channels (depolarizing) to initiate insulin secretion but is sufficient to inhibit repolarizing KCNH6 Kv channels in β cells, we assessed the whole K_V current and APD in mouse primary β cells using patch clamp techniques. K_V currents were elicited by increasing depolarizing pulses with a 10-mV step interval (Figure 7A). As expected, KCNH6 knockout significantly impeded the whole K_V currents in primary islet β cells (Figure 7B and C), and the reduction in K_V currents resulting from the application of E4031 (a KCNH6 inhibitor) disappeared in *Kcnh6*-βKO primary β cells (Figure 7D and E). We then administered 10 μM quinine to islet β cells and observed a significant decrease in the total Kv current density in the WT but not the *Kcnh6*-βKO group (Figure 7F and G), suggesting that low-dose quinine primarily targets KCNH6 to affect whole K_V currents in β cells. K_V currents, which mediate the repolarization process, are tightly associated with the APD of excitable cells. Quinine treatment significantly prolonged the APD of WT β cells (Figure 7H), but did not change that of *Kcnh6*-βKO islet β cells (Figure 7I). These results indicated that low-dose quinine mainly targets KCNH6 to inhibit K_V currents and prolong APD.

Discussion

Severe malaria patients are prone to developing hypoglycemia for multiple reasons, such as the consumption of glucose by Plasmodium and defects in the gluconeogenesis pathway (Homewood, 1977; Dekker et al., 1997). The insulinotropic effect of antimalarials is also a significant cause of hypoglycemia in malaria patients (Davis et al., 1990). Quinine has long been reported to enhance insulin secretion and even cause hypoglycemia in some circumstances (White et al., 1983; Harats et al., 1984; Kerr and Bdiri, 2008; Njomatchoua et al., 2017). The mechanism underlying this insulinotropic effect of quinine is known to involve its direct interaction with the Kir 6.2 subunit to close K_{ATP} channels (Gribble et al., 2000). K_{ATP} channels are the predominant K^+ channels that open at rest in β cells to maintain a hyperpolarized state in the absence of glucose. The closure of K_{ATP} channels, resulting from an elevated ATP/ADP ratio due to glucose metabolism, triggers the depolarization of the plasma membrane, subsequent Ca^{2+} influx, and the release of insulin granules (Gilon et al., 1993). Some drugs, such as sulfonylureas and quinine, can directly block K_{ATP} channels to provoke electrical activity without metabolic stimuli, which may explain how these drugs can cause hypoglycemia (Atwater et al., 1979; Henquin and Meissner, 1982).

The present study showed that low-dose (2.5–20 μM) quinine specifically promoted insulin secretion under high-glucose conditions but had no effects under low-glucose conditions. This phenomenon indicates that low-dose quinine is insufficient to close enough K_{ATP} channels to initiate insulin secretion without adequate metabolic stimuli, but it can enhance high glucose-induced insulin release, which means that in addition to K_{ATP}, quinine may target other ion channels to affect insulin secretion. The K_V family is responsible for repolarizing β cells to terminate insulin secretion (MacDonald and Wheeler, 2003; Herrington et al., 2006; Jacobson et al., 2007). Previous studies have revealed that Kv11.1 (hERG1, KCNH2) and Kv11.2 (hERG2, KCNH6) are abundantly expressed in pancreatic β cells and play critical roles in APD and insulin secretion (Hyltén-Cavallius et al., 2017; Rorsman and Ashcroft, 2018; Yang et al., 2018). In this work, we demonstrated that quinine inhibits both KCNH2 and KCNH6 channels at low micromolar concentrations in transfected HEK293T cells, with the affinity for KCNH6 channels 2 times greater than that for KCNH2 channels.

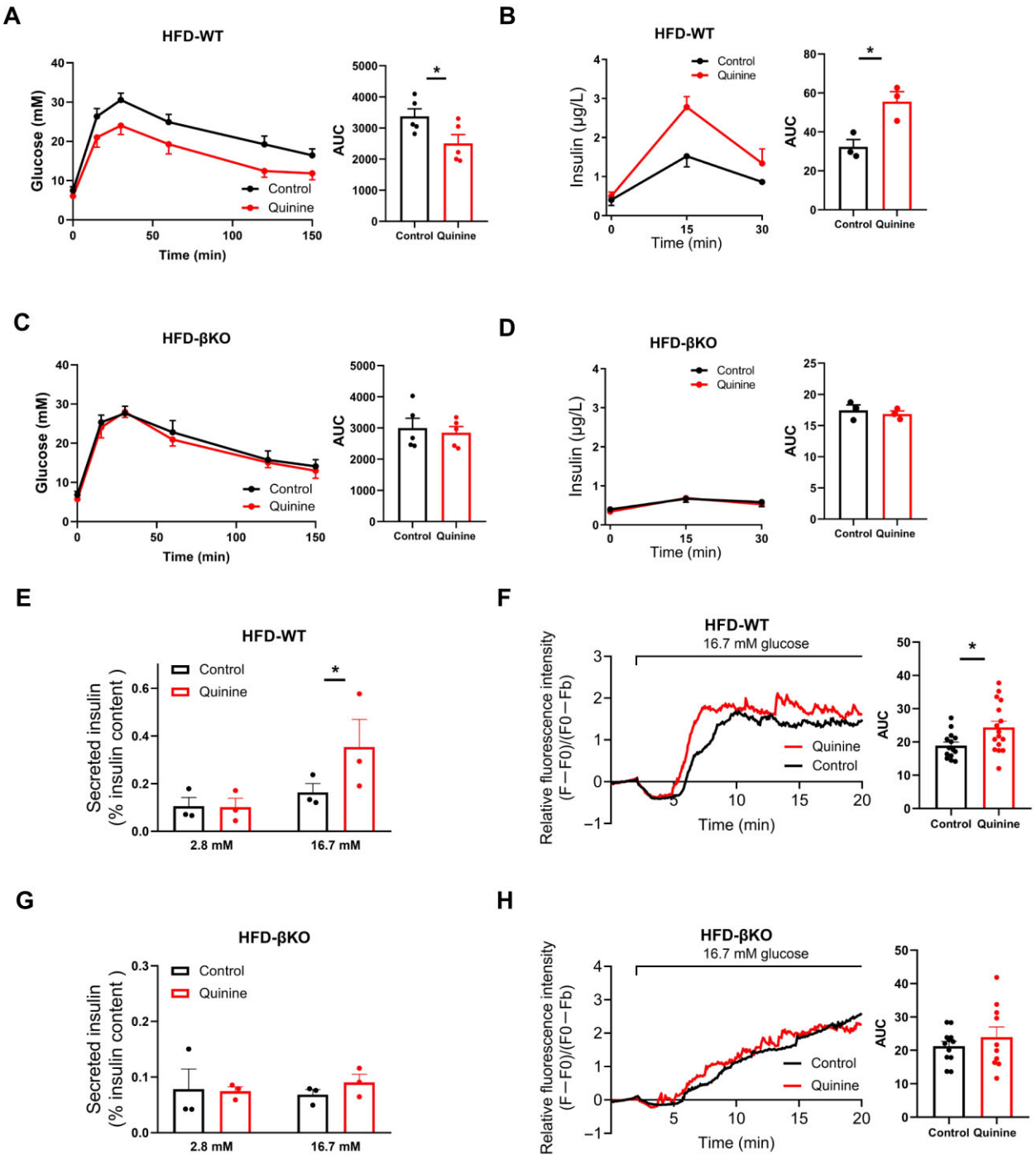

Figure 5 Insulinotropic effect of low-dose quinine on HFD-fed mice. (**A**–**D**) HFD-fed WT and *Kcnh6*-βKO mice received i.p. injection of glucose after 1 h treatment with quinine or vehicle (DMSO). (**A** and **B**) Blood glucose and plasma insulin levels in HFD-fed WT mice. (**C** and **D**) Blood glucose and plasma insulin levels in HFD-fed *Kcnh6*-βKO mice. (**E** and **G**) Normalized secreted insulin levels in islets from HFD-fed WT or *Kcnh6*-βKO mice before and after high-glucose (16.7 mM) stimulation during a GSIS test. (**F** and **H**) Glucose (16.7 mM)-evoked intracellular Ca^{2+} transients in primary β cells from HFD-fed WT or *Kcnh6*-βKO mice. The values are presented as mean ± SEM. *$P < 0.05$. Significance values were calculated using Student's unpaired *t*-test.

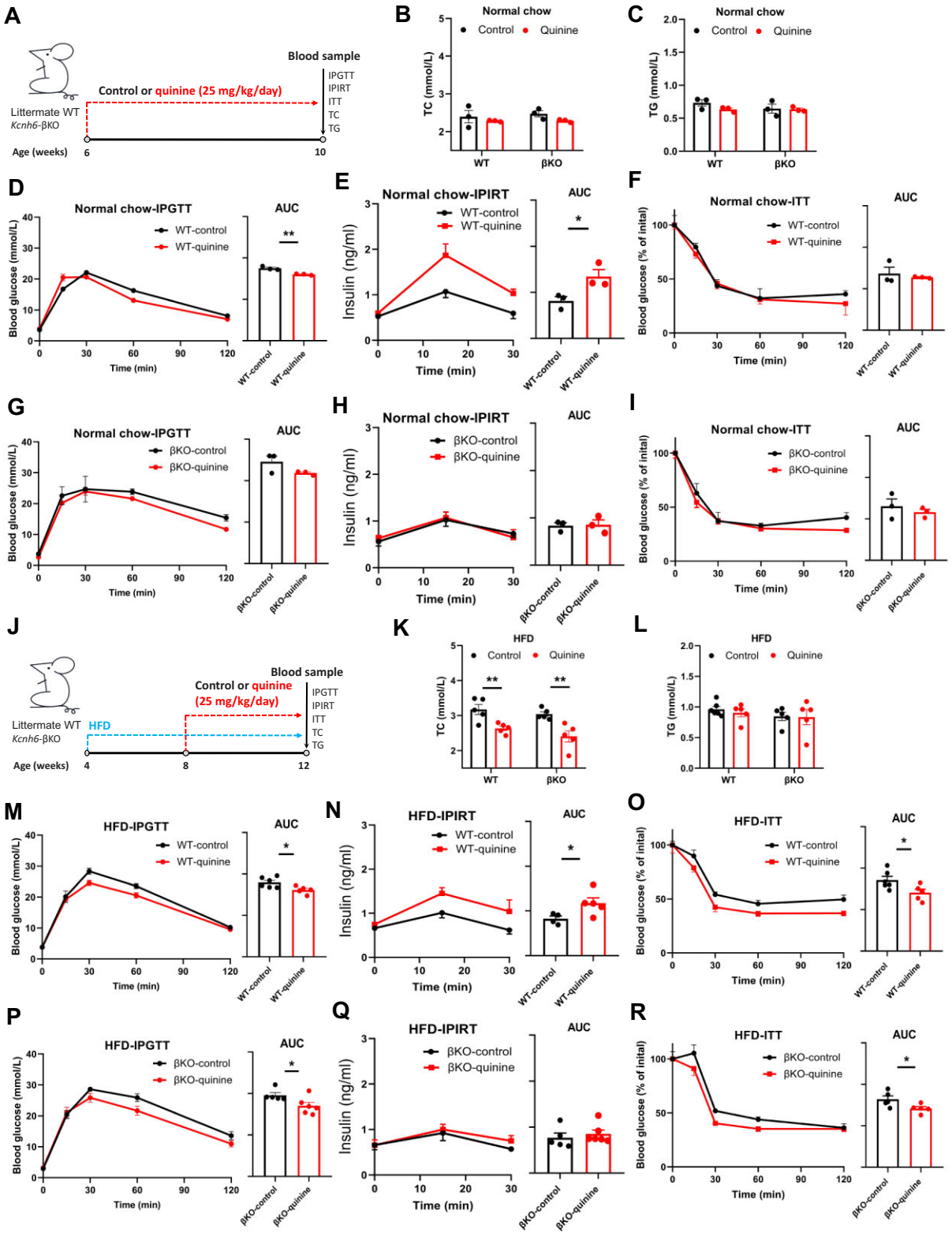

Figure 6 The long-term effects of chronic low-dose quinine administration on metabolic parameters in mice. (**A** and **J**) Flow charts depicting the experimental steps. *Kcnh6*-βKO mice and their WT littermates were fed with a normal chow diet (**A**–**I**) or an HFD (**J**–**R**) and treated with or without low-dose quinine (25 mg/kg of body weight/day) for the indicated periods. At the end of the experiments, IPGTT (**D, G, M,** and **P**), IPIRT (**E, H, N,** and **Q**), ITT (**F, I, O,** and **R**), serum TC (**B** and **K**) and TG (**C** and **L**) measurements were performed. The values are presented as mean ± SEM. $^{*}P < 0.05$ and $^{**}P < 0.01$. Significance values were calculated using Student's unpaired *t*-test.

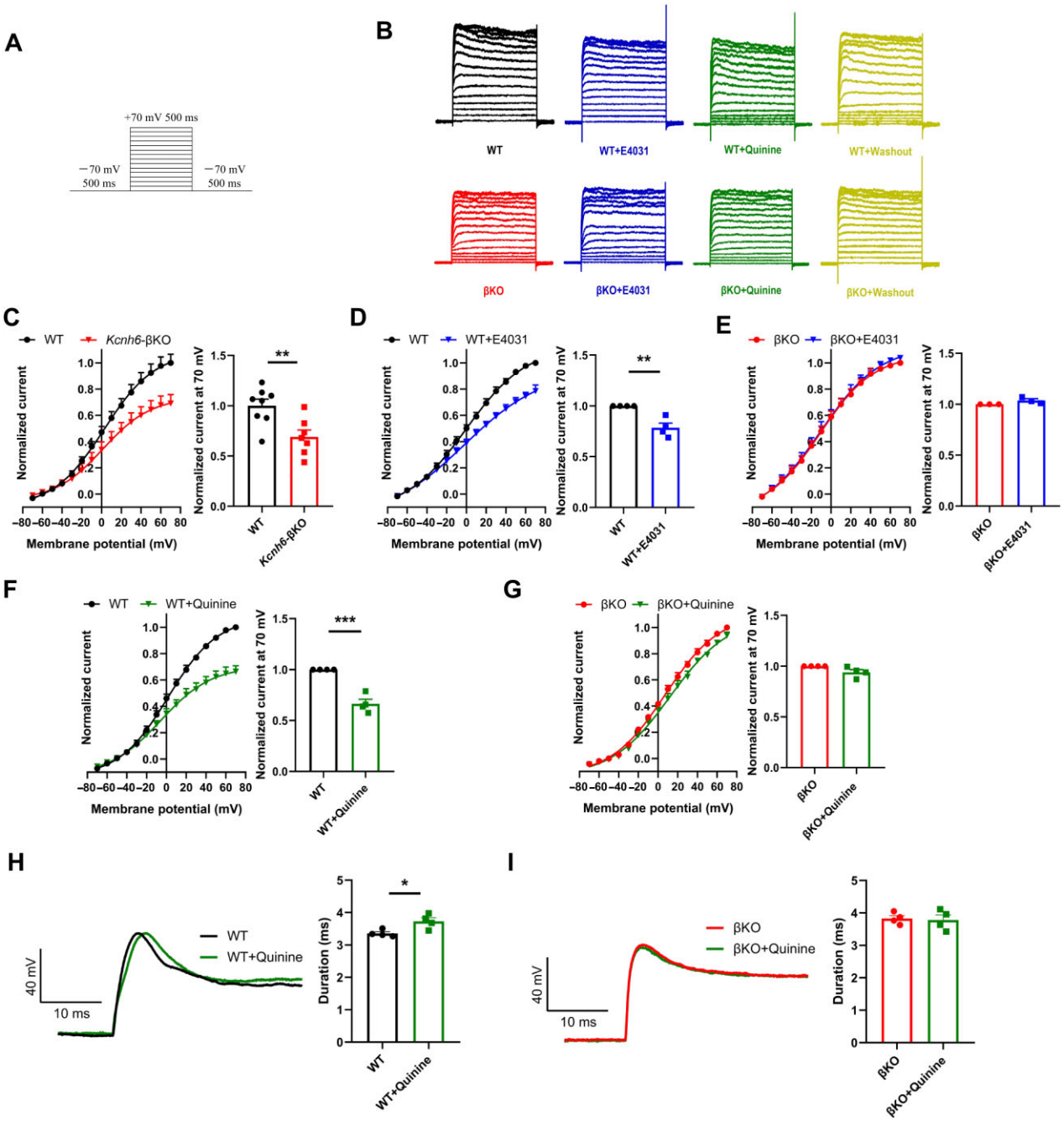

Figure 7 Effects of low-dose quinine on electrophysiological recordings of primary pancreatic β cells. (**A** and **B**) Representative total Kv currents in primary β cells from WT and *Kcnh6*-βKO mice treated with E4031, quinine, or vehicle. (**C**–**G**) Summary of the steady-state I–V curves for Kv currents and the mean of Kv current densities at +70 mV. (**H** and **I**) Representative APDs of primary pancreatic β cells and summary of the mean APD. $n = 4$. The values are presented as mean ± SEM. $^{*}P < 0.05$, $^{**}P < 0.01$, and $^{***}P < 0.001$. Significance values were calculated using Student's unpaired *t*-test.

Next, we performed animal experiments to detect whether quinine can increase insulin secretion through KCNH2 or KCNH6 channel. We found that low-dose (25 mg/kg) quinine cannot induce insulin secretion in fasting mice (without sugar application) but can increase plasma insulin and decrease blood glucose in IPIRTs and IPGTTs (with glucose stimuli), which is in agreement with the *in vitro* islet GSIS test results. The application of low-dose quinine increased the GSIS and glucose-evoked Ca^{2+} influx in *Kcnh2*-βKO mice as well as in WT mice but not in *Kcnh6*-βKO mice, supporting the importance of KCNH6 in the effectiveness of quinine, which may result from the relatively lower affinity of quinine for KCNH2.

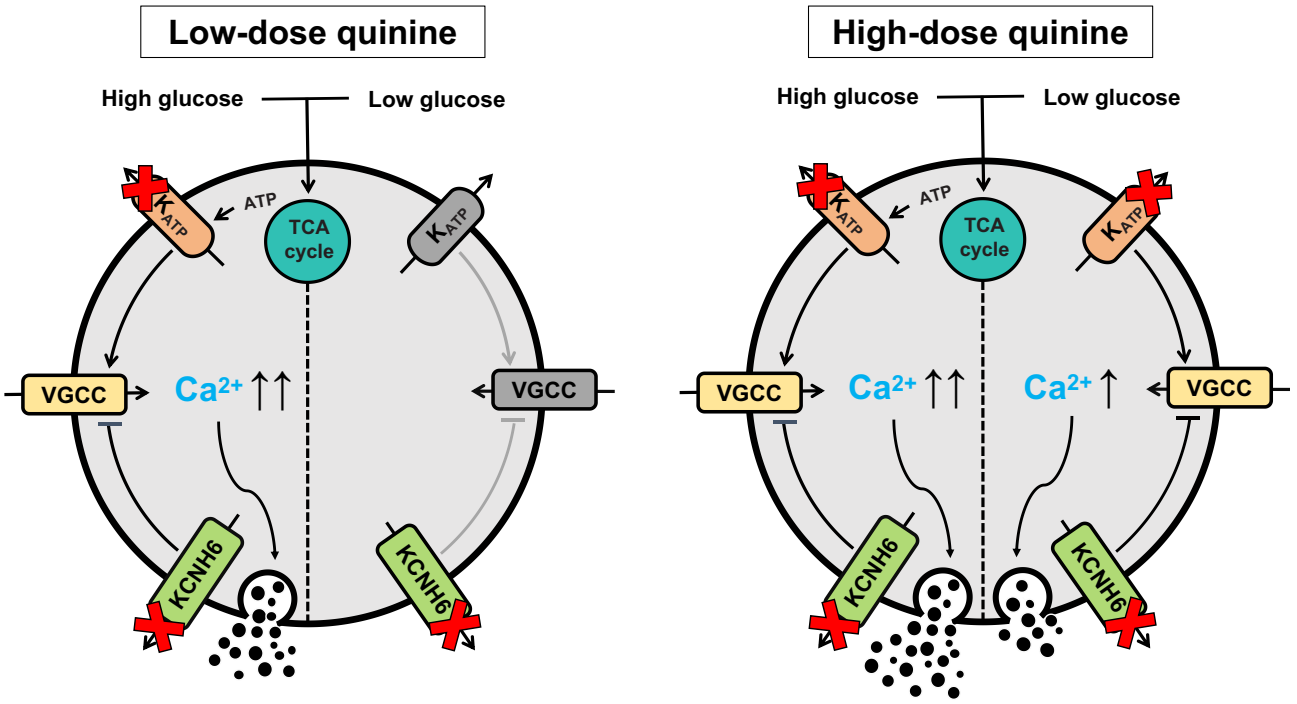

Figure 8 Schematic depicting that low-dose quinine targets KCNH6 to potentiate glucose-induced insulin secretion.

Furthermore, we administered low-dose quinine to chow diet-fed or HFD-fed *Kcnh6*-βKO mice and found that insulin release in response to glucose stimuli was unaffected by quinine application *in vivo* (IPIRT) and *in vitro* (islet GSIS test) in *Kcnh6*-βKO mice. In Ca^{2+} imaging and electrophysiological experiments, the increased glucose-evoked Ca^{2+} spikes and prolonged APD induced by 10 μM quinine were only observed in the β cells from WT but not *Kcnh6*-βKO mice, which explains why insulin secretion was unaffected in *Kcnh6*-βKO mice. Thus, KCNH6 must play a critical role in low-dose quinine-induced potentiation of the GSIS.

Chronic low-dose quinine administration improved glucose tolerance in HFD-fed *Kcnh6*-βKO mice, which was mediated by ameliorated insulin sensitivity rather than enhanced insulin secretion. In addition, the serum TC concentration was reduced in both HFD-fed WT and *Kcnh6*-βKO mice after chronic quinine treatment, indicating that the long-term effects of quinine are independent of KCNH6 knockout. Chloroquine, an analog of quinine, was reported to attenuate diet-induced obesity and glucose intolerance through a mechanism involving FGF-21 (Ortiz-Silva et al., 2023). Whether long-term quinine treatment imparts other metabolic benefits, apart from potentiating insulin secretion, through other targets needs further investigation.

Our previous studies demonstrated that chronic KCNH6 dysfunction results in β cell failure and glucose intolerance with hypoinsulinemia. In this work, the GSIS of *Kcnh6*-βKO islets was severely impaired compared to that of WT controls. To verify that the lack of effects of low-dose quinine on *Kcnh6*-βKO mice is due to KCNH6 knockout rather than poor β-cell health in βKO mice, we applied increasing doses of quinine to *Kcnh6*-βKO islets and proved the reserved function of *Kcnh6*-βKO islets. Nonetheless, further detection in our future work would still be valuable. First, although lower than that of WT controls, the insulin secretion of *Kcnh6*-βKO islets could still be provoked by high-dose quinine, indicating the preserved function of *Kcnh6*-βKO islets. Thus, an immediate gene deletion animal model, such as tamoxifen-treated KCNH6 floxed INS2-Cre/ERT mice, is needed in our future studies to exclude the chronic effects of KCNH6 knockout. Second, considering that KCNH2 is highly expressed in the heart, quinine is still inadequate for use as a safe insulin secretagogue due to its adverse cardiovascular effects, which result from QT interval prolongation caused by KCNH2 inhibition. To eliminate the risk of cardiac toxicity resulting from KCNH2 inhibition, our group has been analyzing the molecular structure of KCNH6 channel through cryo-electron microscopy technique and is trying to conduct a comprehensive analysis of the structural differences between KCNH6 and KCNH2. Based on the structural differences, we plan to develop a KCNH6-specific blocker as a safe insulin secretagogue that rarely targets KCNH2. In addition, as a broad-spectrum K^+ channel blocker, quinine may also promote insulin secretion through other channels. Due to our technical limitations, we only measured the quinine's IC_{50} responses to KCNH2 and KCNH6. In the future, comparing the affinities for different repolarizing K^+ channels and K_{ATP} channels can further clarify the insulinotropic effect of low-dose quinine.

Although high-dose quinine significantly elevated plasma insulin in fasting mice, the blood glucose in the control and some experimental groups unexpectedly increased after

15-min treatment with quinine (or control solution). These contradictory blood glucose changes may be attributed to stress-induced hyperglycemia arising from the irritation caused by oral gavage in mice (Ghosal et al., 2015; Hull et al., 2020).

Overall, the results of our study demonstrated that low-dose quinine targets KCNH6 to potentiate insulin secretion following exposure to high-glucose stimuli (Figure 8), which complements the mechanism underlying quinine-induced insulin secretion and provides new insights into KCNH6-targeted drug development.

Materials and methods

Chemicals

Quinine (HY-D0143) and E4031 (HY-15551) were purchased from MedChemExpress.

Animal model

C57BL/6 J mice were purchased from Weitong Lihua Animal Technology. *Kcnh6*-βKO mice were generated by intercrossing a floxed Kcnh6 mouse line with the rat insulin promoter 2 (RIP2)-driven Cre transgenic mouse line as previously described. RIP2-Cre^{+}:$Kcnh6^{loxp+/+}$ (*Kcnh6*-βKO) mice were generated by PCR genotyping using DNA from tail snips. Littermates with a floxed gene background from the same breeding pair were used as WT controls. *Kcnh2*-βKO mice purchased from Jiangsu GemPharmatech Company were generated using the Cre-LoxP recombinase system. An HFD (60% fat, 20% carbohydrate, and 20% protein in calorie percentage; Research Diets) was provided to mice beginning at 4 weeks of age for 2 months. All mice used in this study were maintained and handled in compliance with the procedures reviewed and approved by the Ethics Review Committee at the Institute of Zoology, Capital Medical University (Beijing, China), according to the ethical guidelines elucidated by the institutional Animal Care and Use Committee (No. TRECKY2018-037).

IPGTT, IPIRT, and ITT

To perform IPGTT and IPIRT, 2 g/kg glucose was injected into mice (i.p.). Blood glucose was measured at 0, 15, 30, 60, and 120 min after glucose injection with an ACCU-CHEK Performa automatic glucometer (Roche). Blood samples were taken from the angular vein at 0, 15, and 30 min after glucose injection. The serum insulin concentration was measured by an ELISA kit (Mercodia). Mice were fasted overnight for the GTT and IRT. Considering an absorption lag-time of ∼1 h before quinine reaches its maximum plasma concentration (Dyer et al., 1994; Pussard et al., 2003), we chose to administer quinine 1 h ahead IPGTTs and IPIRTs to make sure that the drug could sufficiently interact with its targets. To perform ITT, 0.75 units/kg insulin was injected into mice after 4 h fasting. Blood glucose was measured at 0, 15, 30, 60, and 120 min after insulin injection with an ACCU-CHEK Performa automatic glucometer.

TG and TC measurement

Serum TG and TC concentrations were measured by using TG or TC measurement kits (Applygen) according to the supplier recommendations.

Islet and β cell isolation

Islets isolated from the pancreas of mice were digested with collagenase P (Roche) as described previously. Islets were cultured for 24 h before the experiment. To obtain dispersed β cells, the islets were incubated in 0.05% trypsin at 37°C for 5 min, dispersed into single cells, placed on glass-bottom cell culture dishes (NEST), and cultured for 48 h.

Insulin secretion test

Insulin secretion from islets was measured in Krebs–Ringer buffer supplemented with 120 mM NaCl, 5 mM KCl, 24 mM $NaHCO_3$, 2 mM $CaCl_2$, 1 mM $MgCl_2$, 0.1% bovine serum albumin (BSA), 15 mM HEPES (pH 7.4), and glucose at the indicated concentrations. Static GSIS was tested by using 10 islets of comparable size from each group. After 30 min of incubation in low-glucose Krebs–Ringer buffer for adaptation, the islets were transferred to renewed low-glucose (2.8 mM) Krebs–Ringer buffer for 60 min for the basic IRT. Then, we incubated the islets in high-glucose (16.7 mM) Krebs–Ringer buffer for another 60 min to assess insulin secretion under stimulated conditions. Dynamic insulin secretion was monitored by islet perfusion. A total of 40 islets per lane were perfused with low-glucose Krebs–Ringer buffer for 30 min for stabilization and then perfused under basic and stimulated conditions as described at a constant flow rate (1.0 ml/min). Perfusion samples were collected at the indicated intervals. All islets were collected and lysed for total insulin content measurement to normalize the results. The insulin concentration in the samples was assayed using an ELISA kit (Mercodia).

Cells

All cells were cultured in an environmentally controlled incubator with a humidified atmosphere composed of 95% air and 5% CO_2 at 37°C. HEK293T cells were cultured in Dulbecco's modified Eagle medium supplemented with 10% fetal bovine serum (FBS) and 1% penicillin–streptomycin. Pancreatic islets and primary pancreatic β cells were cultured in RPMI 1640 medium supplemented with 10% FBS and 1% penicillin–streptomycin. Lipofectamine 3000 reagent (Invitrogen) was used to transiently transfect HEK293T cells according to the manufacturer's protocol.

Cell viability experiment

HEK293T cells and primary pancreatic β cells were incubated with different concentrations of quinine for 24 h. The effects of quinine on cell viability and cytotoxicity were examined using an MTT assay kit (Invitrogen) according to the manufacturer's protocol.

Time-lapse imaging

Primary pancreatic β cells prepared for Ca^{2+} imaging were loaded with 4 μM Fluo-4 AM (Invitrogen) and 0.1% pluronic F-127 (Beyotime) dissolved in low-glucose Krebs–Ringer buffer according to the manufacturer's protocol. The fluorescence intensity was determined with a DeltaVision Ultra system (GE). High-glucose Krebs–Ringer buffer was added at the indicated times to induce depolarization and Ca^{2+} influx. Images were acquired at 4-sec intervals. The ImageJ software was used for fluorescence intensity measurements.

Electrophysiology

A whole-cell patch clamp experiment was performed as previously described (Lu et al., 2024). For recording the currents of KCNH6 or KCNH2 channels, transfected HEK293T cells were elicited with 4-sec depolarizing pulses ranging from −60 mV to +60 mV and 4-sec repolarizing pulses to −40 mV. Kv currents were determined at a stable potential of −70 mV and then recorded while the current was increased from −70 mV to +70 mV in increments of 10 mV. APD was determined with 0.5-nA current stimulation for 50 ms using primary pancreatic islet β cells.

Western blotting

Collected cells were first lysed in RIPA Lysis Buffer (Beyotime). Equivalent amounts of protein samples were loaded into 10% or 12% TGX Stain-Free polyacrylamide gels (Bio-Rad) and separated by electrophoresis. The proteins were transferred to polyvinylidene fluoride membranes (Millipore), which were then blocked with NcmBlot Blocking Buffer (NCM Biotech) at room temperature for 15 min. The membranes were incubated with primary antibodies overnight at 4°C, followed by incubation with diluted secondary antibodies for 2 h at room temperature. Signals were detected by enhanced chemiluminescence (Bio-Rad). ImageJ software was used for densitometry measurements.

Data analysis

Statistical analyses were conducted by using GraphPad Prism (version 8.0). Data are presented as mean ± standard error of the mean (SEM), and statistical comparisons were made with the unpaired-sample *t*-test. $P < 0.05$ was considered to indicate statistical significance.

Acknowledgements

The authors thank the participants and staff of the studies for valuable contributions.

Funding

This work was supported by grants from the National Natural Science Foundation of China (82070890 to J.L. and 81930019 to J.-K.Y.) and Beijing Natural Science Foundation (7232230 to J.L.).

Conflict of interest: none declared.

Author contributions: J.-K.Y. and J.L. conceived and designed the study. F.-R.X. and J.L. designed and performed the experiments, analyzed the data, and wrote the draft of the manuscript. All authors interpreted the data, revised the manuscript, and approved the final version. J.-K.Y. is the guarantor of this work.

References

Achan, J., Talisuna, A.O., Erhart, A., et al. (2011). Quinine, an old anti-malarial drug in a modern world: role in the treatment of malaria. Malar. J. *10*, 144.

Atwater, I., Dawson, C.M., Ribalet, B., et al. (1979). Potassium permeability activated by intracellular calcium ion concentration in the pancreatic β-cell. J. Physiol. *288*, 575–588.

Bryan, J., Crane, A., Vila-Carriles, W.H., et al. (2005). Insulin secretagogues, sulfonylurea receptors and K_{ATP} channels. Curr. Pharm. Des. *11*, 2699–2716.

Davis, T.M., Karbwang, J., Looareesuwan, S., et al. (1990). Comparative effects of quinine and quinidine on glucose metabolism in healthy volunteers. Br. J. Clin. Pharmacol. *30*, 397–403.

Dekker, E., Hellerstein, M.K., Romijn, J.A., et al. (1997). Glucose homeostasis in children with falciparum malaria: precursor supply limits gluconeogenesis and glucose production. J. Clin. Endocrinol. Metab. *82*, 2514–2521.

Dierich, M., van Ham, W.B., Stary-Weinzinger, A., et al. (2019). Histidine at position 462 determines the low quinine sensitivity of ether-à-go-go channel superfamily member kv 12.1. Br. J. Pharmacol. *176*, 2708–2723.

Dyer, J.R., Davis, T.M., Giele, C., et al. (1994). The pharmacokinetics and pharmacodynamics of quinine in the diabetic and non-diabetic elderly. Br. J. Pharmacol. *38*, 205–212.

Fatherazi, S., and Cook, D.L. (1991). Specificity of tetraethylammonium and quinine for three K channels in insulin-secreting cells. J. Membr. Biol. *120*, 105–114.

Fedida, D. (1997). Gating charge and ionic currents associated with quinidine block of human Kv1.5 delayed rectifier channels. J. Physiol. *499 (Pt 3)*, 661–675.

Fedida, D., Bouchard, R., and Chen, F.S. (1996). Slow gating charge immobilization in the human potassium channel Kv1.5 and its prevention by 4-aminopyridine. J. Physiol. *494 (Pt 2)*, 377–387.

Ghosal, S., Nunley, A., Mahbod, P., et al. (2015). Mouse handling limits the impact of stress on metabolic endpoints. Physiol. Behav. *150*, 31–37.

Gilon, P., Shepherd, R.M., and Henquin, J.C. (1993). Oscillations of secretion driven by oscillations of cytoplasmic Ca^{2+} as evidences in single pancreatic islets. J. Biol. Chem. *268*, 22265–22268.

Gribble, F.M., Davis, T.M., Higham, C.E., et al. (2000). The antimalarial agent mefloquine inhibits ATP-sensitive K-channels. Br. J. Pharmacol. *131*, 756–760.

Harats, N., Ackerman, Z., and Shalit, M. (1984). Quinine-related hypoglycemia. N. Engl. J. Med. *310*, 1331.

Henquin, J.C. (1982). Quinine and the stimulus–secretion coupling in pancreatic β-cells: glucose-like effects on potassium permeability and insulin release. Endocrinology *110*, 1325–1332.

Henquin, J.C., and Meissner, H.P. (1982). Opposite effects of tolbutamide and diazoxide on $^{86}Rb^{+}$ fluxes and membrane potential in pancreatic B cells. Biochem. Pharmacol. *31*, 1407–1415.

Herrington, J., Zhou, Y.-P., Bugianesi, R.M., et al. (2006). Blockers of the delayed-rectifier potassium current in pancreatic β-cells enhance glucose-dependent insulin secretion. Diabetes *55*, 1034–1042.

Homewood, C.A. (1977). Carbohydrate metabolism of malarial parasites. Bull. World Health Organ. *55*, 229–235.

Hull, R.L., Hackney, D.J., Giering, E.L., et al. (2020). Acclimation prior to an intraperitoneal insulin tolerance test to mitigate stress-induced hyperglycemia in conscious mice. J. Vis. Exp. https://doi.org/10.3791/61179

Hyltén-Cavallius, L., Iepsen, E.W., Wewer Albrechtsen, N.J., et al. (2017). Patients with long-QT syndrome caused by impaired hERG-encoded Kv11.1 potassium channel have exaggerated endocrine pancreatic and incretin function associated with reactive hypoglycemia. Circulation *135*, 1705–1719.

Jacobson, D.A., Kuznetsov, A., Lopez, J.P., et al. (2007). Kv2.1 ablation alters glucose-induced islet electrical activity, enhancing insulin secretion. Cell Metab. *6*, 229–235.

Jacobson, D.A., and Philipson, L.H. (2007). Action potentials and insulin secretion: new insights into the role of kv channels. Diabetes Obes. Metab. *9 (Suppl 2)*, 89–98.

Jones, R.G., Sue-Ling, H.M., Kear, C., et al. (1986). Severe symptomatic hypoglycaemia due to quinine therapy. J. R. Soc. Med. *79*, 426–428.

Kerr, D., and Bdiri, A. (2008). Quinine-associated hypoglycaemia causing diabetes. Diabet. Med. *25*, 241–242.

Lu, J., Zhao, R.-X., Xiong, F.-R., et al. (2024). All-potassium channel CRISPR screening reveals a lysine-specific pathway of insulin secretion. Mol. Metab. *80*, 101885.

MacDonald, P.E., and Wheeler, M.B. (2003). Voltage-dependent K^+ channels in pancreatic β cells: role, regulation and potential as therapeutic targets. Diabetologia *46*, 1046–1062.

Malin, S.A., Guo, W.X., Jafari, G., et al. (1998). Presenilins upregulate functional K^+ channel currents in mammalian cells. Neurobiol. Dis. *4*, 398–409.

Misler, S., Barnett, D.W., Gillis, K.D., et al. (1992). Electrophysiology of stimulus–secretion coupling in human β-cells. Diabetes *41*, 1221–1228.

Misler, S., Gee, W.M., Gillis, K.D., et al. (1989). Metabolite-regulated ATP-sensitive K^+ channel in human pancreatic islet cells. Diabetes *38*, 422–427.

Njomatchoua, A.C., Tankeu, A.T., Sobngwi, E., et al. (2017). Glycemic effects of quinine infusion in healthy volunteers. BMC Res. Notes *10*, 423.

Ortiz-Silva, M., Leonardi, B.F., Castro, É., et al. (2023). Chloroquine attenuates diet-induced obesity and glucose intolerance through a mechanism that might involve FGF-21, but not UCP-1-mediated thermogenesis and inhibition of adipocyte autophagy. Mol. Cell. Endocrinol. *578*, 112074.

Proks, P., Reimann, F., Green, N., et al. (2002). Sulfonylurea stimulation of insulin secretion. Diabetes *51 Suppl 3*, S368–S376.

Proverbio, M.C., Mangano, E., Gessi, A., et al. (2013). Whole genome SNP genotyping and exome sequencing reveal novel genetic variants and putative causative genes in congenital hyperinsulinism. PLoS One *8*, e68740.

Pussard, E., Bernier, A., Fouquet, E., et al. (2003). Quinine distribution in mice with Plasmodium berghei malaria. Eur. J. Drug Metab. Pharmacokinet. *28*, 11–20.

Rorsman, P., and Ashcroft, F.M. (2018). Pancreatic β-cell electrical activity and insulin secretion: of mice and men. Physiol. Rev. *98*, 117–214.

Saadeh, K., Nantha Kumar, N., Fazmin, I.T., et al. (2022). Anti-malarial drugs: mechanisms underlying their proarrhythmic effects. Br. J. Pharmacol. *179*, 5237–5258.

Shi, W., Wymore, R.S., Wang, H.S., et al. (1997). Identification of two nervous system-specific members of the erg potassium channel gene family. J. Neurosci. *17*, 9423–9432.

White, N.J., Warrell, D.A., Chanthavanich, P., et al. (1983). Severe hypoglycemia and hyperinsulinemia in falciparum malaria. N. Engl. J. Med. *309*, 61–66.

Yang, J.-K., Lu, J., Yuan, S.-S., et al. (2018). From hyper- to hypoinsulinemia and diabetes: effect of KCNH6 on insulin secretion. Cell Rep. *25*, 3800–3810.e6.

Received July 2, 2024. Revised October 27, 2024. Accepted January 22, 2025.